

ULTRASONIC INVESTIGATION OF MACRO RESIDUAL STRESSES IN 15Cr2NMFA STEEL AFTER UNIAXIAL COMPRESSION

*O.I. Zaporozhets, S.A. Kotrechko, N.A. Dordienko, V.A. Mykhailovsky, A.V. Zatsarnaya
G.V. Kurdyumov Institute for Metal Physics of the N.A.S. of Ukraine, Kiev, Ukraine*

Precise measurements of bulk-wave ultrasonic velocity in orthogonal directions were executed in specimens made of the 15Cr2NMFA steel after uniaxial compression (UC) for $\varepsilon=0\dots60\%$. Based on the obtained data and theoretical computations, the residual macro-stresses (RMS) for different strain values were calculated with accounting for the texture contribution. The coefficients of orientation distribution of crystallites (texture coefficients W_{4i0}) were determined and pole figures were constructed, by which the relative intensity of diffraction lines ($\Delta I_{(ijk)}$) for the main crystallographic directions was ascertained. The peculiarities in strain dependences of the researched quantities were found and explanations to the observed effects were given.

It is known that the plastic deformation of metals can give rise to internal oriented micro- and macrostresses (OrMS), which significantly influence their mechanical properties under repeated loading. However, opposite views on the magnitude and sign of these stresses were expressed by some authors. Thus, in [1] it was established on the basis of X-ray studies that the sign of OrMS is opposite to that of external deforming stresses. On the contrary, in [2, 3] it was shown, that OrMS are always compressed independently of external stresses. These contradictions could be related to the drawbacks of the X-ray measurement techniques and experimental data processing. The authors of [4], in their opinion, took into account these shortcomings of their predecessors and showed that both single and alternating plastic deformation of heterogeneous alloys results in triaxial OrMS with a sign opposite to the last deformation. In [5] the authors found and discussed the effect of changes in the mechanisms of brittle fracture – from transcrystalline for undeformed RPV steel 15Cr2MFA to intercrystalline one after plastic deformation by compression, which may also be related to the formation of residual stress state in alloys. Residual macro-stresses (RMS) in various metal aggregates were studied by many experts using ultrasonic (US) method (see e.g. [6–11] and cited references therein). To realize the last, acoustic elasticity phenomenon was used, which is based on the dependence of the elastic moduli and the corresponding velocities of ultrasonic on the magnitude and direction of macrostresses acting on the section of specimen (detail, product) tested by sonic. Both the ability to scan specimen by ultrasonic beam and possibility to diagnose its stress state not only in the surface layers, but also in its volume is an important advantage of the US method. In [12, 13] to study spatial distribution of RMS in specimens of polycrystalline chromium subjected to thermal cycling pretreatment (TCT), the method of UNDT of macro-stresses in abnormal materials was used [14]. This method is based on the dependence of the phase transformation temperature (for Cr this is Neel temperature T_N) and the corresponding US abnormalities on the sum of diagonal components of macrostress tensor (σ_{ii}). To obtain the dependence of σ_{ii} on the coordinate of section of the specimen tested by sonic, the temperature dependence of the ultrasonic velocity was recorded at each site, and

the value of σ_{ii} was determined by displacement of $v(T)$ minimum relatively to its position in the initial specimen. On the same specimens, RMS in the surface layers were determined by X-ray technique, and a complete diagram of RMS in chrome after TCT was built. Based on these results, it was shown that residual stresses in the volume and on the surface of treated specimen differ in magnitude and have the opposite sign. In case of change in the size of stressed specimen, for instance, by etching, a redistribution of RMS occurs, and error in determining of the latter increases. The results of [12, 13] indicate the difficulty of estimation of the stress state in the specimen (detail, product) volume only by the data obtained from the surface layers. The aim of this work was to research with the US method the residual stress state in the volume of specimens of the steel 15Cr2NMFA after plastic deformation by uniaxial compression (UC) using the effect acoustic elasticity. For this purpose, precise measurements of longitudinal (v_l) and transverse (v_t) velocity of US in orthogonal directions, and the density (ρ) in the initial and deformed specimens were executed in the work. Based on the obtained data for different strains (ε) with accounting for the texture contribution, RMSs were calculated. Also, the coefficients of orientation distribution of crystallites (texture coefficients W_{4i0}) were determined, and the pole figures (PF) were built, by which the relative intensity of diffraction lines ($\Delta I_{(ijk)}$) for the main crystallographic directions of textured specimens was ascertained.

THEORETICAL FUNDAMENTALS

Determination of uni-, bi- and triaxial macro-stresses (MS) in polycrystalline aggregates by measuring the US velocity was shown in many works [6–11, 15–16]. Only the case with uniaxial MS briefly considered below accounting for above problem.

According to [8], for the direction of the US wave propagation (orientation of its wave vector is \vec{k}) in the isotropic specimen parallelly to direction of the applying uniaxial macro-stresses ($\vec{k} \parallel \vec{\sigma}$):

$$\rho v_l^2 = \lambda + 2\mu + \frac{\sigma}{3K} \left[2l + \lambda + \frac{(\lambda + \mu)}{\mu} (4m + 4\lambda + 10\mu) \right], \quad (1)$$

$$\rho v_i^2 = \mu + \frac{\sigma}{3K} \left[m + \frac{\lambda n}{4\mu} + 4\lambda + 4\mu \right]. \quad (2)$$

In the direction normal to the direction of acting stresses ($\vec{k} \perp \vec{\sigma}$):

$$\rho v_l^2 = \lambda + 2\mu + \frac{\sigma}{3K} \left[2l - \frac{2\lambda}{\mu} (m + \lambda + 2\mu) \right], \quad (3)$$

$$\rho v_{t1}^2 = \mu + \frac{\sigma}{3K} \left[m + \frac{\lambda n}{4\mu} + \lambda + 2\mu \right], \quad (4)$$

$$\rho v_{t2}^2 = \mu + \frac{\sigma}{3K} \left[m - \frac{(\lambda + \mu)n}{2\mu} - 2\lambda \right], \quad (5)$$

where σ is positive for tensile stresses and negative for compressive stresses, $t1$ and $t2$ are transverse wave polarized along ($\vec{s} \parallel \vec{\sigma}$) and normally ($\vec{s} \perp \vec{\sigma}$) to the direction of applying stresses, respectively, λ , μ is Lamé constants for an isotropic solid (material); l , m , n are the third-order Murnaghan constants, $K = \lambda + \frac{2}{3}\mu$ - hydrostatic compression modulus, ρ is the density of material in unstressed (unloaded) state.

From (2) it can be seen that the transverse US velocity in the direction of the applied stresses does not depend on the orientation of the polarization vector \vec{s} , which means that macro-stresses in other directions are absent.

From the equations (4) and (5), within the first order approximation of σ , one can obtain:

$$\sigma = \frac{2\mu}{1 + n/4\mu} \times \frac{v_{t1} - v_{t2}}{\langle v_{t1,2} \rangle}, \quad (6)$$

where $\langle v_{t1,2} \rangle$ is transverse velocity in the unstressed (unloaded) state, which can be substituted by (with) the expression $\frac{v_{t2} + v_{t1}}{2}$. Accounting for the texture contribution (the second term of the numerator in parentheses):

$$\sigma = \frac{\rho[(v_{t1}^2 - v_{t2}^2) - (v_{t1o}^2 - v_{t2o}^2)]}{1 + n/4\mu}, \quad (7)$$

where v_{t1o} and v_{t2o} are corresponding transverse velocities in the unstressed (unloaded) textured aggregate. Or, similarly to (6):

$$\sigma \approx \frac{2\mu}{1 + n/4\mu} \times \left(\frac{v_{t1} - v_{t2}}{\langle v_{t1,2} \rangle} - \frac{v_{t1o} - v_{t2o}}{\langle v_{t1o,2o} \rangle} \right), \quad (8)$$

Analysis of published data and own research results of the authors of this work have exhibited that the texture contribution of the transverse and Rayleigh velocity of sound to anisotropy is by the order of magnitude higher than the contribution from residual macroscopic stresses in the steel. This fact causes the importance of using a theoretical basis for selection of velocities in expressions such as (7) and (8) depending on a specific experimental situation.

US TECHNIQUE FOR TEXTURE ANALYSIS OF ANISOTROPIC POLYCRYSTALS

The technique is also described in details in e.g. [17–19], and it is widely used in modern scientific and industrial laboratories. The method is based on the concept of a textured aggregate as a quasi-monocrystal with lower crystallographic symmetry compared with the crystallites.

Fig. 1 presents a schematic view of the rolled specimen that have the shape of rectangular parallelepiped in an orthogonal coordinate system with six possible for measuring transverse (v_{ij}) ultrasonic velocities ($i, j = 1, 2, 3$). Axis 1 denotes the rolling direction (RD), 2 – the transverse direction (TD) and 3 – the direction of deformation (normal direction, ND). The 1-st index of v_{ij} indicates the direction of propagation, and 2-nd indicates the direction of polarization vector of US wave in the specimen.

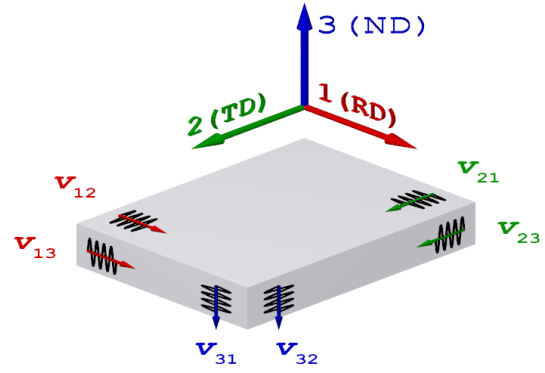


Fig. 1. Schematic view of the rolled specimen for measurement of US volume velocities and texture analysis of anisotropic polycrystals

In addition to the transverse velocities in orthogonal directions, it is possible to measure three longitudinal velocities of US (v_{ii}). Uniaxial compression is a special case of rolling deformation with equivalent axes 1 and 2, which enables to use above theoretical basis for the case of the UC.

Relationship between the effective elastic coefficients (C'_{ij}), corresponding sound velocities (v_{ij}) and required (unknown) texture coefficients (W_{ijk}) for cubic polycrystals can be represented by the following expressions:

$$C'_{11} = \rho v_{11}^2 = K + \frac{4}{3}\mu + \quad (9)$$

$$+ C^a \frac{12}{35} \sqrt{2\pi^2} \left(W_{400} - \frac{2}{3} \sqrt{10} W_{420} + \frac{1}{3} \sqrt{70} W_{440} \right),$$

$$C'_{22} = \rho v_{22}^2 = K + \frac{4}{3}\mu + \quad (10)$$

$$+ C^a \frac{12}{35} \sqrt{2\pi^2} \left(W_{400} + \frac{2}{3} \sqrt{10} W_{420} + \frac{1}{3} \sqrt{70} W_{440} \right),$$

$$C'_{33} = \rho v_{33}^2 = K + \frac{4}{3}\mu + C^a \frac{32}{35} \sqrt{2\pi^2} W_{400}, \quad (11)$$

$$C'_{44} = \rho v_{23,32}^2 = \mu - C^a \frac{16}{35} \sqrt{2} \pi^2 \left(W_{400} + \sqrt{\frac{5}{2}} W_{420} \right), \quad (12)$$

$$C'_{55} = \rho v_{13,31}^2 = \mu - C^a \frac{16}{35} \sqrt{2} \pi^2 \left(W_{400} - \sqrt{\frac{5}{2}} W_{420} \right), \quad (13)$$

$$C'_{66} = \rho v_{12,21}^2 = \mu + C^a \frac{4}{35} \sqrt{2} \pi^2 \left(W_{400} - \sqrt{70} W_{440} \right), \quad (14)$$

$$C'_{23} = K - \frac{2}{3} \mu - C^a \frac{16}{35} \sqrt{2} \pi^2 \left(W_{400} + \sqrt{\frac{5}{2}} W_{420} \right) = \quad (15)$$

$$= K - \frac{5}{3} \mu + C'_{44},$$

$$C'_{13} = K - \frac{2}{3} \mu - C^a \frac{16}{35} \sqrt{2} \pi^2 \left(W_{400} - \sqrt{\frac{5}{2}} W_{420} \right) = \quad (16)$$

$$= K - \frac{5}{3} \mu + C'_{55},$$

$$C'_{12} = K - \frac{2}{3} \mu + C^a \frac{4}{35} \sqrt{2} \pi^2 \left(W_{400} - \sqrt{70} W_{440} \right) = \quad (17)$$

$$= K - \frac{5}{3} \mu + C'_{66},$$

where C^a is anisotropy factor, which is calculated using the elastic coefficients of crystallites. Index a denotes the averaging method: ($a=V$) is averaging by Voigt, ($a=R$) – by Royce and ($a=H$) – by Voigt-Royce-Hill. Herewith

$$C^V = C_{11} - C_{12} - 2C_{44}, \quad (18)$$

$$C^R = \frac{50(C_{11} - C_{12} - 2C_{44})(C_{11} - C_{12})C_{44}}{[3(C_{11} - C_{12}) + 4C_{44}]^2}, \quad (19)$$

$$C^H = \frac{C^V + C^R}{2}, \quad (20)$$

where C_{11} , C_{12} and C_{44} are the elastic constants of monocrystal of material.

In the expressions (12) – (14)

$$v_{ij,ji} = \frac{v_{ij} + v_{ji}}{2} \quad (i, j = 1, 2, 3)$$

are the transverse US velocities averaged over symmetric indices. Inequality $v_{ij} \neq v_{ji}$ indicates the presence of current or residual macrostresses in a material [15, 16]:

$$\sigma = \rho(v_{ij}^2 - v_{ji}^2). \quad (21)$$

Therefore, in the case of uniaxial compression of specimens, according to the Fig. 1, expression (7) can be written as:

$$\sigma_3 = \frac{\rho[(v_{i3}^2 - v_{ij}^2) - (\langle v_{i3,3i}^2 \rangle - \langle v_{ij,ji}^2 \rangle)]}{1 + n/4\mu}, \quad (22)$$

where index 3 at σ denotes the direction of UC and RMS; $i=1,2; j=2,1; \langle v_{i3,3i} \rangle \approx \frac{v_{i3} + v_{3i}}{2}$ and

$$\langle v_{ij,ji} \rangle \approx \frac{v_{12} + v_{21}}{2}.$$

Pole figures according to the coefficients W_{400} , W_{420} and W_{440} , which are calculated by three US velocities

selected from equations (9)–(14), are built using expressions [20]:

$$q(\zeta, \eta) = 1/4 + S_4 \left[P_4^0(\zeta) W_{400} + P_4^2(\zeta) W_{420} \cos 2\eta + P_4^4(\zeta) W_{440} \cos 4\eta \right] + S_6 \left[P_6^0(\zeta) W_{600} + P_6^2(\zeta) W_{620} \cos 2\eta + P_6^4(\zeta) W_{640} \cos 4\eta + P_6^6(\zeta) W_{660} \cos 6\eta \right], \quad (23)$$

where $S_4 = S_6 = 2\pi$ for the pole figure (100); $S_4 = -\pi/2$, $S_6 = -13\pi/4$ for the pole figure (110); $S_4 = -4\pi/3$, $S_6 = -32\pi/9$ for the pole figure (111). In this case, the terms with coefficient W_{6j0} are neglected because of their relative smallness.

TECHNIQUE AND THE OBJECTS OF INVESTIGATION

On the first stage of preparation the specimens were cut out as cylinders of height $h=30$ mm and diameter $d=25$ mm from the fragment of VVER-1000 wall, which were subjected to a preliminary UC at room temperature till strains $\varepsilon=10, 20, 30, 40, 50$ and 60%. Thereafter, the specimens in the form of a rectangular parallelepiped with dimensions $10 \times (8 \dots 10) \times (8 \dots 10)$ mm were made from them. One of directions 3 coincided with UC direction. Directions 1 and 2 were normal to corresponding planes of specimen. Ultrasonic measurements at frequencies of 10...30 MHz by automated device, the same as was employed in [21, 22], were executed. The time of delay of echo signal (τ), by the magnitude of which and by length of which acoustic path, the US velocity was determined, was measured by fixing of passing through zero value of the specified period of high-frequency filling of US radio pulse from the specimen. The absolute instrumental error of τ measurement did not exceed 1 ns, and the relative one was less than above by the order of magnitude. The corresponding error of measurement of ultrasonic velocity was 10^{-4} rel. units on a time base of 10 μ s. The density of the specimens was measured by the differential method of hydrostatic weighing using quartz or germanium etalon with the error of 10^{-4} rel. units at the specimen weight of 10 g. Residual stresses were determined by anisotropy of the transverse ultrasonic velocity in directions normal to the applying UC and compensating textural contribution to the RMS was estimated by averaging of the measured velocities over symmetric indices. Applied software enabled to assess the relative intensity of the diffraction lines $\Delta I_{[ijk]} = I_{[ijk] \max} - I_{[ijk] \min}$ when constructing pole figures.

RESULTS AND DISCUSSION

Strain dependences of the specimen density (ρ), the relative changes in the longitudinal ($\Delta v_{ii}/v_{ii0}$) and transverse ($\Delta v_{ij}/v_{ij0}$) ultrasonic velocity along and across the UC, and their anisotropy are presented in Figs. 2 and 3.

It is evident that after deformation by UC all the US velocities and density are decreased compared to their initial values. The greatest UC effect is observed on the first (up to $\varepsilon \leq 10 \dots 30\%$) stages of deformation. At higher ε , influence of strain weakens, and the US

velocities grow with increase in ϵ , but remain less than their initial values. Anisotropy of v_l and v_t also depends on the strain value anomalously. On the one hand this anisotropy is a measure of macro-stresses in the material [6, 7], and on the other hand, it may be associated with texture formed and changing during deformation [8, 10, 11]. It was ascertained, that the US transverse velocity along the UC (v_{3j}) direction doesn't show any anisotropy for rotation of polarization vector in the plane normal to the direction of strain, which indicates the absence of residual stresses in other geometric directions. At propagation of transverse US waves normally to the UC, a significant anisotropy of v_{ij} and its dependence on the direction of the polarization vector \vec{s} and strain ϵ was observed. In the case of the orientation \vec{s} along of UC direction ($ij=23, 13$) changes in v_t with increase in ϵ are significantly greater than those for transverse velocity with a polarization in direction normal to the UC ($ij=12, 13, 21, 23$).

The latter is related to specific features of forming of the axial texture in specimens during their deformation (results are given below).

Fig. 4 represents residual macro-stresses along the axis of 3 for various values of ϵ calculated by (22). Herewith, the calculation was carried out using transverse velocities of ultrasonic, v_{ij} , in directions 1 and 2 (Fig. 1) with the polarization along and across to UC action.

Fig. 4 also presents the average values of these stresses. In the calculations, the measured values of $\rho=7.830 \text{ g/cm}^3$ and $\mu=83.889 \text{ GPa}$ and the Murnaghan's coefficient for steel $n=643.5 \text{ GPa}$ [8] were used.

It is evident that the uniaxial compression of investigated specimens gives rise to the appearance of tensile residual stresses in their volume, which increase with increase in strain, reach their maximum at $\epsilon=30\%$, and decrease at $\epsilon>30\%$. According to the authors, observed non-monotonic dependence of $\sigma_3(\epsilon)$ is due to partial relaxation of the RMS caused by changes in the mechanism of metal deforming at high strains.

It should be noted that at $\epsilon=60\%$, significant scatter of σ_3 values, associated with the experimentally observed spatial inhomogeneity of OMS in these specimens takes place. Selective X-ray tests of the same specimens after the UC have shown that compressive RMS appear in their surface layers.

Fig. 5 exhibits typical pole figures [100] and [111] for initial and deformed by UC specimens of 15Cr2NMFA steel from deformation plane for $\epsilon=0, 10, 30, 50\%$. In addition to ϵ , the values of texture coefficients W_{410} and relative intensity of the diffraction lines $\Delta I_{[ijk]}=I_{[ijk]_{max}}-I_{[ijk]_{min}}$ are given in interlinear inscriptions. For W_{410} calculations, the measured values $\rho=7.830 \text{ g/cm}^3$; $\mu=83.889 \text{ GPa}$; $K=168.585 \text{ GPa}$ and $C_{11}=232.2 \text{ GPa}$; $C_{12}=135.6 \text{ GPa}$; $C_{44}=119.0 \text{ GPa}$ from [8] are used. Thus, $C^H=-139.99 \text{ GPa}$. It is evident that at the early stages of deformation the axial texture is formed in specimens, degree of texturing of which, unlike the dependence of $\sigma_3(\epsilon)$, changes slightly at $\epsilon \geq 20 \dots 30\%$.

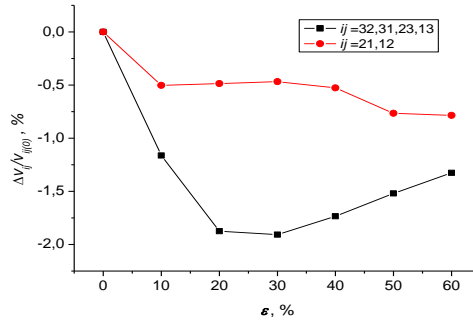
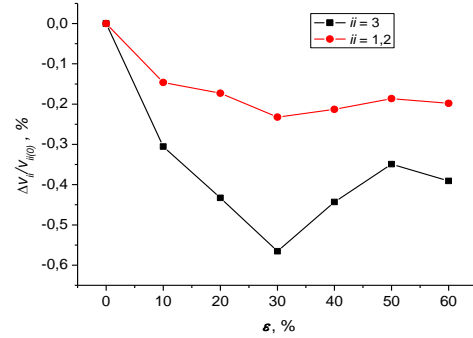
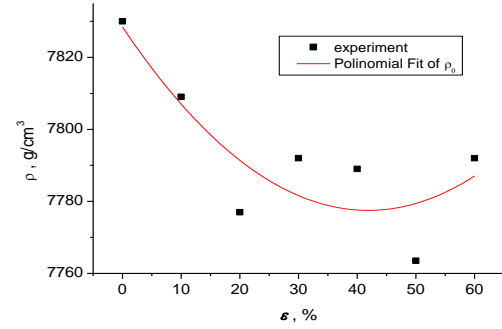


Fig. 2. Strain dependences of density (ρ) and changes of longitudinal (v_{ii}) and transverse (v_{ij}) US velocity along and across the UC (direction 3) relatively to their values in the undeformed state for specimens of 15Cr2NMFA steel

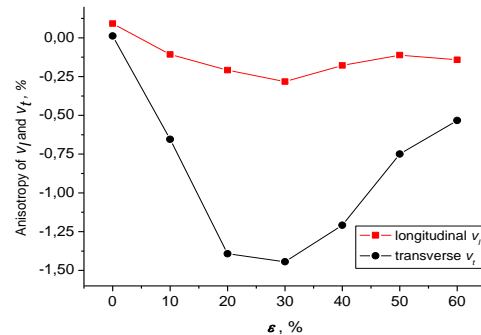


Fig. 3. Dependence of anisotropy of averaged longitudinal $(v_{33}-\langle v_{11,22} \rangle)/\langle v_{ii} \rangle$ and transverse $2(v_{t \min}-v_{t \max})/(v_{t \min}+v_{t \max})$ ultrasonic velocities in the specimens of 15Cr2NMFA steel on strain

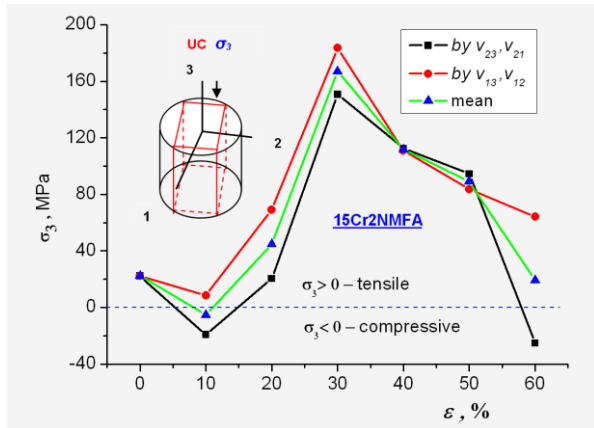


Fig. 4. Dependence of RMS σ_3 in 15Cr2NMFA steel on ϵ . The calculation was executed using the transverse US velocity in the direction normal to the UC accounting for the contribution of texture. Insertions: a schematic view of the specimen; US velocity v_{ij} employed in the calculation

Above is confirmed by Fig. 6, in which the dependences of $\Delta I_{[ijk]}(\epsilon)$ for the main crystallographic directions of investigated specimens obtained from the corresponding pole figures are shown. This result agrees with the parallel X-ray tests, the results of which will be presented in another work.

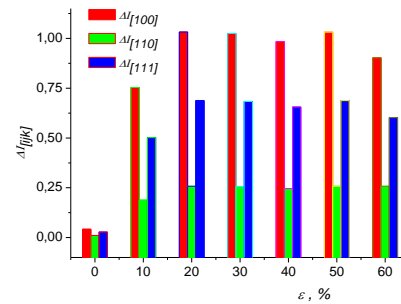


Fig. 6. The relative intensity of the diffraction lines $\Delta I_{[ijk]}$ for directions [100], [110] and [111] for 5Cr2NMFA steel at UC depending on strain ϵ

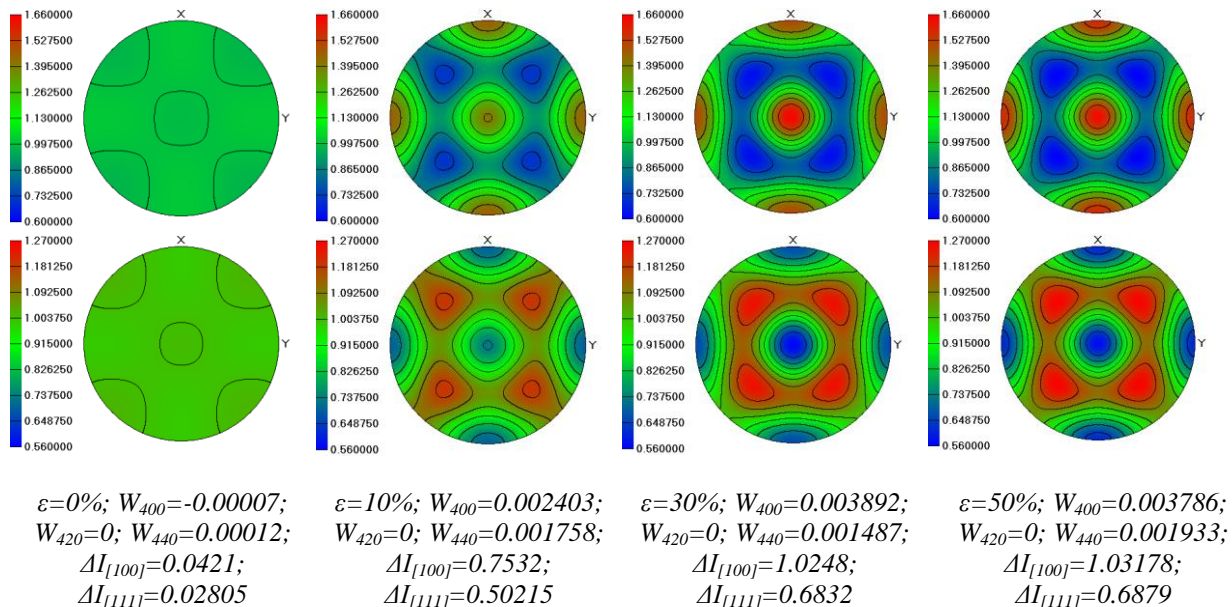


Fig. 5. Pole figures [100] (upper group of PF) and [111] (lower group of PF) for an initial and deformed by UC 15Cr2NMFA steel from the deformation plane. The values of ϵ , coefficients W_{4i0} and relative intensity of the diffraction lines $\Delta I_{[ijk]}$ are given in captions (interlinear inscriptions)

CONCLUSIONS

As a result of precise measurements of both longitudinal (v_l) and transverse (v_t) US velocities in orthogonal directions, as well as of the density (ρ), in specimens made of steel 15Cr2NMFA, deformed by uniaxial compression (UC) for strain $\epsilon=0-60\%$, the anomalous changes in v_l , v_t and their anisotropy depending on ϵ were ascertained. Based on the obtained evidence and theoretical computations, the residual macro-stresses (RMS) for different strains with taking into account of the texture contribution were calculated. The coefficients of orientation distribution of crystallites (texture coefficients W_{4i0}) were also determined and pole figures were constructed, by which the relative intensity of diffraction lines ($\Delta I_{[ijk]}$) for the main

crystallographic directions was ascertained. It is shown that in the volume of specimens, RMS after UC are tensile ones, and their dependence on the strain value has a maximum close to $\epsilon=30\%$. It is found that for initial stages of deformation ($\epsilon=10-20\%$) in specimens, the axial texture is formed that at further deformation changes insignificantly. Such non-monotonic dependence of $\sigma(\epsilon)$ is explained by a partial relaxation of the RMS at $\epsilon>30\%$.

REFERENCES

1. А. Тейлор. Рентгеновская металлография. М.: «Металлургия», 1965, 387 с.
2. Д.М. Васильев. О микронапряжениях, возникающих в поликристаллических образцах при

- пластическом деформировании // *ЖТФ*. 1958, т. 28, №11, с. 25-27.
3. Д.М. Васильев. О природе эффекта Баушингера // *Некоторые проблемы прочности твердого тела*. М.: Изд-во АН СССР, 1959, с. 37-48.
4. Ю.В. Бойко, И.В. Навроцкий, В.В. Куколь. Зависимость ориентированных микронапряжений в пластически деформированной стали от направления внешней нагрузки // *ФММ*. 1984, т. 57, №5, с. 77-80.
5. Б.З. Марголин, В.А. Швецова, А.Я. Варовин. Предварительное сжатие материалов как фактор смены механизма хрупкого разрушения ОЦК-металлов // *Проблемы прочности*. 1996, №4, с. 5-18.
6. А.Н. Гузь, Ф.А. Махорт. *Введение в акустоупругость*. Киев: «Наукова думка», 1977, 151 с.
7. В.М. Бобренко, М.С. Вангели, А.Н. Куценко. *Акустические методы контроля напряженного состояния материала машин*. Кишинев: «Штиница», 1981, 148 с.
8. D.R. Allen, C.M. Sayers. The Measurement of Residual Stress in Textured Steel Using an Ultrasonic Velocity Combinations Technique // *Ultrasonics*. 1984, v. 22, N 4, p.179-188.
9. Ф.А. Махорт, О.И. Гуца. Основы теории определения трехосных напряжений ультразвуковым методом // *Прикладная механика*. 1987, т. 23, №1, с. 18-23.
10. A.V. Clark, H. Fukioka, D.V. Nitrakovic, J.C. Noulder. Ultrasonic characterization of residual stress and texture in cast steel railroad wheels // *Rev. Progr. Quant Nondestruct. Eval. V. 6B: 2nd half Proc. 13th Annu. Rev. Progr. Quant. Nondestruct. Eval. Zayolla: Calif. Aug. 3-8, 1986. New York, London*. 1987, p. 1567-1575.
11. Н.Е. Никитина. *Акустоупругость. Опыт практического применения*. Н. Новгород: «ТАЛАМ», 2005, 208 с.
12. О.И. Запорожец, Л.В. Тихонов. Ультразвуковые исследования распределения остаточных микронапряжений в хроме после термоциклической обработки // *Металлофизика. Письма в редакцию*. 1985, т. 7, №5, с. 119-120.
13. О.И. Запорожец, Л.В. Тихонов. Новый ультразвуковой метод неразрушающего контроля чистоты и напряженного состояния металлов и сплавов // *Высокочистые вещества*. 1994, №3, с. 100-103.
14. А. с. 1126866 М. Кл. 01 29/00. *Ультразвуковой способ контроля микронапряжений в изделиях* / В.Н. Гриднев, О.И. Запорожец, Л.В. Тихонов. Оpubл. в БИ, 1984, №44.
15. C.M. Sayers, G.P. Clarke. Effect of non-alignment of specimen and texture axes on the measurement of stress using the ultrasonic SH wave technique // *J. Phys. D: Appl. Phys.* 1986, v. 19, p. 1547-1553.
16. C.M. Sayers, G.G. Proudfoot. Angular dependence of the ultrasonic SH wave velocity in rolled metal sheets // *J. Mech. Phys. Solids*. 1986, v. 36, N 6, p. 579-592.
17. C.M. Sayers. Ultrasonic Velocities in Anisotropic Polycrystalline Agregates // *J. Phys. D: Appl. Phys.* 1982, v. 15, p. 2157-2167.
18. J. Lewandowski. Evaluation of the Texture of Polycrystalline Agregate from Ultrasonic Measurements // *Ultrasonics*. 1986, v. 24, N 2, p.73-80.
19. R.B. Thompson, J.F. Smith, S.S. Lee, G.C. Jonson. A Comparison of Ultrasonic and X-Ray Determinations of Texture in Thin Cu and Al Plates // *Met. Trans. A*. 1989, v. 20A, p. 2431-2439.
20. M. Hirao, N. Hara. Ultrasonic Pole Figure for the Texture of Aluminium Alloy // *Appl. Phys. Lett.* 1987, v. 50, N 20, p. 1411-1412.
21. О.И. Запорожец, Н.А. Дордиенко, А.В. Бочко, Г.С. Доронин, Н.Н. Кузин, И.А. Петруша. Исследование упругих модулей ПСТМ типа DBN, ПТНБ и гексантил-Р импульсным УЗ-методом // *Перспективные материалы. Труды I Международной конференции «Functional Nanomaterials and High-Purity Substances»*. М.: «Интерконтакт Наука», 2008, №6, в. 1, с. 152-158.
22. В.М. Ажажа, Н.А. Дордиенко, О.И. Запорожец, О.П. Карасевская, К.В. Ковтун, В.А. Михайловский, С.П. Стеценко, А.П. Шпак. Ультразвуковая диагностика эволюции текстуры при прокатке сплава Zr1Nb // *Труды XIX Международной конференции по физике радиационных явлений и радиационному материаловедению (XIX-ICRP)*, 06-11 сентября 2010 г., Алушта, Крым, 2010, с. 145-146.

Article received 16.06.2014

УЛЬТРАЗВУКОВЫЕ ИССЛЕДОВАНИЯ ОСТАТОЧНЫХ МАКРОНАПРЯЖЕНИЙ В СТАЛИ 15Х2НМФА ПОСЛЕ ОДНООСНОГО СЖАТИЯ

О.И. Запорожец, С.А. Котречко, Н.А. Дордиенко, В.А. Михайловский, О.Б. Зацарная

Выполнены прецизионные измерения объемных скоростей ультразвука (УЗ) в образцах из стали 15Х2НМФА в ортогональных направлениях после одноосного сжатия (ОС) на степень деформации $\varepsilon=0...60\%$. На основе полученных данных и использованной теоретической базы рассчитаны остаточные микронапряжения (ОМН) для разных ε с учетом текстурного вклада. Определены коэффициенты распределения ориентаций кристаллитов (текстурные коэффициенты W_{4i0}) и построены полюсные фигуры, по которым определена относительная интенсивность дифракционных линий ($\Delta I_{[ijk]}$) для главных кристаллографических направлений. Выявлены особенности в зависимостях исследованных величин от ε и дано объяснение наблюдаемым эффектам.

УЛЬТРАЗВУКОВІ ДОСЛІДЖЕННЯ ЗАЛИШКОВИХ МАКРОНАПРУЖЕНЬ У СТАЛІ 15X2НМФА ПІСЛЯ ОДНОВІСНОГО СТИСКАННЯ

О.І. Запорожець, С.О. Котречко, М.О. Дордієнко, В.А. Михайловський, О.В. Зацарна

Виконані прецизійні вимірювання об'ємних швидкостей ультразвуку (УЗ) в ортогональних напрямках зразків зі сталі 15X2НМФА після одновісного стискання (ОС) на ступінь деформації $\varepsilon=0\dots60\%$. На основі отриманих даних та використаної теоретичної бази, розраховані залишкові макронапруження (ЗМН) для різних ε з урахуванням текстурного внеску. Визначено коефіцієнти розподілу орієнтацій кристалітів (текстурні коефіцієнти W_{4i0}) та побудовані полюсні фігури, за якими визначена відносна інтенсивність дифракційних ліній ($\Delta I_{[ijk]}$) для головних кристалографічних напрямків. Виявлено особливості в залежностях досліджених величин від ε і надано пояснення спостережуваним ефектам.